Austrian Journal of Earth Sciences | Vienna | 2017 | Volume 110/1 | 101 - 108 | DOI: 10.17738/ajes.2017.0007

Petrographic coded model concept for the correlation between geomechanical and elastic properties and its application on log data for Alpine rocks

Nina GEGENHUBER[1)*)], Thomas SCHIFKO[2)] & Gerhard PITTINO[3)]

[1)] Montanuniversitaet Leoben, Chair of Applied Geophysics, Franz-Josef-Strasse 18, 8700 Leoben, Austria;

[2)] Fugro Austria GmbH, Einoedstrasse 13, 8600 Bruck an der Mur, Austria;

[3)] Montanuniversitaet Leoben, Chair of Subsurface Engineering, Franz-Josef-Strasse 18, 8700 Leoben, Austria;

[*)] Corresponding author, nina.gegenhuber@unileoben.ac.at

KEYWORDS uniaixal compression strength; compressional wave velocity; petrographic code; logging data; alpine rocks

Abstract

The derivation of geomechanical properties, like the rock strength, from elastic properties is an important topic not only in the oil industry, but also for geothermal projects, tunnelling or mining. It is one of the crucial parameters for the stability of the borehole, the drilling rate or stability of an underground mine. The idea of applying the petrographic model concept which involves an additional mineralogical influence was developed for the correlation between compressional wave velocity and uniaxial compression strength for sandstone, limestone, anhydrite and gypsum. The first step of this model is to define or assume the solid matrix properties of the dense host material, which covers therefore the influence of the rock type/lithology. The second step implements fractures/cracks with an inclusion model. Samples are selected from the surface and from borehole. A newly measurement set-up was developed to measure velocities during the uniaxial compression test. Additionally, the application of the derived equations on log data is tested. The presented correlations using the petrographic coded model concept shows good first results. Correlation between uniaxial compression strength and compressional wave velocity can be derived using the petrographic coded model concept (inclusion and defect model). The derived equations can easily be applied on log data and also deliver good results for the uniaxial compression strength in the borehole.

Die Ableitung geomechanischer Parameter, wie die Gesteinsfestigkeit, von elastischen Eigenschaften, ist nicht nur in der Ölindustrie, sondern auch für Geothermie Projekte, im Tunnelbau oder im Bergbau, von großem Interesse. Es ist eine der Kerngrößen für die Stabilität des Bohrlochs, der Bohrgeschwindigkeit oder der Stabilität eines Untertagebergbaues. Die Idee der Anwendung des petrographisch kodierten Modelkonzeptes, welches zusätzlich den Mineraleinfluss beinhaltet, wurde für die Korrelation zwischen Kompressionswellengeschwindigkeit und einaxialer Druckfestigkeit für Sandstein, Kalkstein, Anhydrit und Gips entwickelt. Der erste Schritt dieses Models ist es, die Matrixwerte von der dichten Materialmasse, welche den Einfluss des Gesteinstyps/der Lithologie beinhaltet, zu bestimmen oder anzunehmen. Der zweite Schritt implementiert Risse/Brüche mit einem Inklusionsmodel. Es wurden Oberflächenproben und Bohrkerne ausgewählt. Ein neuer Messaufbau wurde entwickelt um Geschwindigkeiten währen eines einaxialen Druckversuches zu messen. Zusätzlich wurde die Anwendung der abgeleiteten Gleichungen an Bohrlochdaten getestet. Die hier präsentierten Korrelationen unter Verwendung des petrographisch kodierten Models zeigen erste gute Ergebnisse. Korrelationen zwischen einaxialer Druckfestigkeit und Kompressionswellengeschwindigkeit können mit dem Model (Inklusionen und Defekt Model) abgeleitet werden. Die Gleichungen können weiter leicht an Bohrlochdaten angewendet werden und erste Ergebnisse liefern gute Werte für die einaxiale Druckfestigkeit im Bohrloch.

1. Introduction

The derivation of geomechanical properties from elastic properties is an important topic not only in the oil industry, but also for geothermal projects, tunnelling or mining. Rock strength and the stress field itself cannot be measured directly in the boreholes or on the surface, but is one of the crucial parameters for the stability of the borehole, the drilling rate (penetration rate and the right drill bits) or stability of an underground mine.

Therefore, a lot of research focuses on this problem using different approaches correlating static and dynamic properties. A first good overview for geomechanical properties in the oil industry is given in the book of Fjaer et al. (2008), which covers physical backgrounds, measuring methods, models, correlations and applications of geomechanical properties. Heerden (1987) published a general equation for the correlation between static and dynamic Young's modulus. Many papers can be found focusing on a correlation between petrophysical (geophysical) and geomechanical properties, the measurements itself or models for a derivation of geomechanical properties (e.g. Chen and Hu 2001, Altindag 2012, Karami et al. 2012 or Bhuiyan et al. 2013).

For example Najibi et al. (2015), presented a study on limestone data from Iran and give an additional overview of published equations. Chang et al. (2006) also give an overview of

31 empirical equations for the correlation between uniaxial compression strength (UCS) and physical properties, like compressional wave velocity (vp), modulus and porosity. Chen and Hu (2001) give linear trends for engineering properties like compressional and shear wave velocity and UCS of weak sandstones and Hongkui et al. (2001) use not only sandstone but also limestone, shale, granite, tuff, rhyolite and mudstone for the correlation between dynamic and static Young's modulus and Poisson ratio. Sedimentary rock types are analysed by Altindag (2012) focusing on UCS and vp. A multi-linear regression analysis including tensile strength for the correlation was presented. Oyler et al. (2008) used coal measure rocks for their correlation between UCS and vp with an exponential equation. The relationship between static and dynamic properties for Xishan Rock Cliff Statue is published by Jiang and Sun (2011). Further linear correlations between UCS and vp are given by Karami et al. (2012) for limestone data. A compilation of empirical relationships was published by Schoen (2015).

Other papers cover different approaches for the measurements itself, for example Plona and Cook (1995), who carried out measurements on sandstones or Mashinskii (2004) used dolomite samples for his study. A triaxial measurement set up was used by Fortin et al. (2005) for sandstone samples.

All publications have one thing in common: they try to find correlations between static and dynamic properties (e.g. Young's modulus or Poisson ratio). Therefore, the idea of the application of the petrographic model concept which covers an additional mineralogical influence was developed for the correlation for sandstone, limestone, anhydrite and gypsum. This influence is important because most empirical correlations are based on a specific rock type or geological formation. The application of this model concept delivered excellent results for the correlation between thermal conductivity and compressional wave velocity (Gegenhuber and Schoen, 2014; Gegenhuber and Kienler, 2017). Additionally, there is a focus on the application of the derived equations on log data, which should help to keep it practical. The following chapters will give a short introduction on the samples and the measuring method, followed by the model calculations and their results and last but not least the application on log data.

2. Method

2.1 Samples

Selected samples for this study are taken from outcrops as well as from boreholes in Austria. Various lithologies (limestone, sandstone, gypsum and anhydrite) were included to make a possible petrographic code visible. We used:

- two different Lithothamnium limestone samples (Eocene), which were taken from two different wells in the upper part of the Molasse Basin. "Leitha" limestones (Miocene) from a quarry in St. Margarethen (Burgenland, Austria) are additionally used.
- Sandstone samples are from the limnic series, the Hall Formation as well as from the Puchkirchen Formation (mainly Oligocene-Miocene) also from the Molasse basin and additionally Triassic Buntsandstein samples are taken from a quarry.
- Gypsum and anhydrite are taken from a quarry at Gössl (Styria, Austria) which is part of the Upper "Hallstätter" Nappes (Northern Calcareous Alps) in the Haselgebirge Formation (Permian).

These rock types were selected because they could cover reservoir rocks as well as cap rocks for the oil industry and for geothermal projects. Samples which are measured in the petrophysics laboratory have a diameter of 2.5 cm and a length

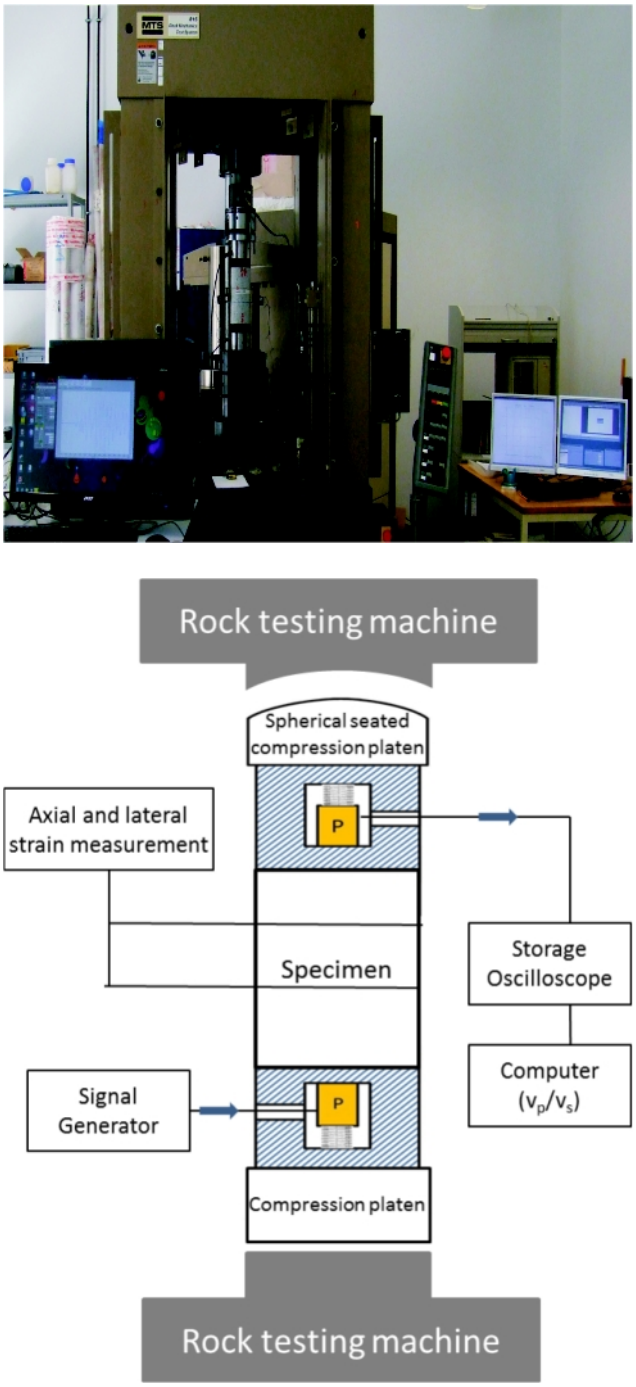

Figure 1: Experimental Set-up: left: picture from the geomechanical laboratory, right: schematic overview of the measurement set-up (p=probes)

of 2.2 cm. In contrast for the geotechnical measurements bigger samples are needed. Most samples have a diameter of 10cm and a length of 200cm, because length should be 2 or 2.5 times the diameter. Table with measured data can be found in the results chapter.

2.2 Measuring Method

Two fundamental properties were measured in the laboratory: Elastic wave velocity using ultrasonic technique and uniaxial compression strength using geomechanics standard technique. The machine-constructional part of the experimental set-up was planned that probes (vp) from the company „Geotron Elektronik" (Pirna, Germany) were not exposed to the high forces during the uniaxial compression test (see figure 1). With this set-up forces up to 2500 kN could be controlled.

The measuring method corresponded to standard measurements in the petrophysics laboratory. A singular mechanical impulse having a frequency of 250 kHz produced by a signal generator was sent through the sample. The arriving signal got forwarded to a storage oscilloscope and to a computer. A self-made program (Gegenhuber and Steiner-Luckabauer 2012) detected the first arrival of the two waves and calculated the wave velocities with the length of the specimen and including dead time. The dead time is the time of the signal through the probes without any sample. The signal was stored at the corresponding pressure stage and afterwards interpreted. Additionally, for the first evaluation of the results an aluminum specimen was tested in the petrophysics laboratory and in the geomechanical laboratory using the newly developed set-up. Both provided the same results. Measurements in the petrophysics laboratory were carried out with a bench-top ultrasonic instrument, where the sample got fixed between transducer and receiver with a contact agent and a pressure of 2 bar. A singular mechanical impulse using 80kHz was produced and sent through the sample. Signal was again furthermore forwarded to the storage oscilloscope and the computer, where it became analyzed.

For the measurements during the uniaxial compression strength test, a cylindrical rock sample was positioned between the two pressure plates, in which the probes were integrated. For an optimal result and uniform stress state an additional spherical mounted pressure plate next to the fixed pressure plate was used. The sensors for the axial and radial changes were directly applied on the specimen. At the beginning the specimen became loaded with a low axial pressure and all sensors, except of the load cell, were adjusted. The following pressure stages were used and were hold for the required measuring time of a few minutes in kN: 50, 100, 150, 200, 350, 500 and vice versa (Pittino et al. 2015).

Additionally, for a fully petrophysical evaluation, plugs (diameter = 2.5 cm, length = 2.2 cm) are taken from the cores and effective porosity, grain and bulk density, compressional (vp) and shear (vs) wave velocities are measured in the laboratory under laboratory conditions. The effective porosity is determined with the principle of Archimedes as well as with a helium pycnometer, which additionally delivers the grain density.

2.3 Model Calculations

The idea of the petrographic coded model concept was first developed for the correlation between thermal conductivity and compressional wave velocity (Gegenhuber and Schoen 2012). A model concept was developed which can express on the one hand effective properties of the solid components determined by the mineral composition (petrographic code) and on the other hand influence of fluid components (pores and fractures) mathematically by model equations. The pores and fractures are implemented with an inclusion model and

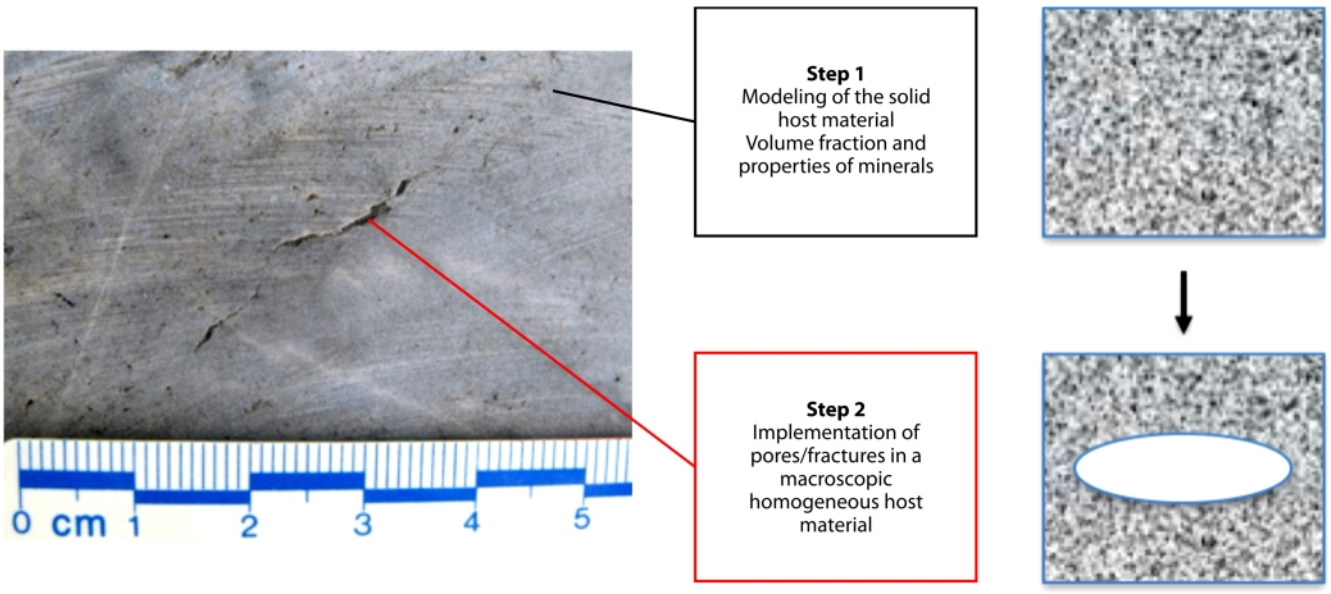

Figure 2: Schematic illustration of the inclusion and defect model and the basic principle including the solid host material, which refers to the mineral composition without any pores or cracks.

a defect model. Starting this new study presented here, the idea of using the same model concept was born, when the first data were evaluated for different lithologies.

Therefore, the same principle is now applied to demonstrate the correlation between uniaxial compression strength and compressional wave velocity.

2.3.1 Inclusion Model

The first approach was the application of the inclusions model (Figure 2) by Budiansky and O'Connell (1976) to calculate compressional wave velocity. This inclusion model has random oriented inclusions assuming a penny-shaped crack medium, which covers all pores, vugs and fractures in a sample. The approach assumes high frequencies (ultrasonic laboratory measurements) for fluid saturated rocks, idealizes ellipsoidal inclusions, isotropic and linear elastic rock matrix and that the cracks are isolated with respect to fluid flow. They derived with a self-consistent algorithm an equation for the elastic properties.

Compressional modulus k_{sc} and shear modulus μ_{sc} (sc refers to the self-consistent approach) result for the inclusion model by Budiansky and O'Connell as:

$$k_{sc} = k_s \cdot \left[1 - \frac{16}{9} \cdot \frac{1-\nu_{sc}^2}{1-2\cdot\nu_{sc}} \cdot \varepsilon\right] \quad (1)$$

$$\mu_{sc} = \mu_s \cdot \left[1 - \frac{32}{45} \cdot \frac{(1-\nu_{sc})\cdot(5-\nu_{sc})}{2-\nu_{sc}} \cdot \varepsilon\right] \quad (2)$$

ε is a "crack density parameter"

$$\varepsilon = \left(\frac{N}{V}\right) \cdot r^3 \quad (3)$$

defined as the number of cracks (N) per unit volume (V) times the crack radius (r) cubed, k_s is the compression modulus for the solid material (=mineral substance without any pores or cracks), ν_{sc} is the Poisson's ratio and μ_s is the shear modulus for the solid material (Mavko et al., 2009). The crack porosity is

$$\Phi = \left(\frac{4\pi}{3}\right) \cdot \alpha \cdot \varepsilon \quad (4)$$

and results with the effective Poisson's ratio in:

$$\nu_{sc} \sim \nu_s \cdot \left(1 - \left(\frac{16}{9}\right) \cdot \varepsilon\right) \quad (5)$$

where ν_s refers for the Poisson ratio of the solid host material and α is the aspect ratio (= α=c/a = length/width of the inclusion). Assumed for the calculations is only α for each rock type. Porosity steps to calculate the correlations are between 0 and 0.5[-].

Table 2 shows input parameters for the calculations. The aspect ratio doesn't strongly influence the correlations here. Data are mainly taken from the literature and adopted to the measured data.

The next step was to test different correlation equations for v_p and *UCS* from the literature, due to the fact that *UCS* cannot be calculated with any inclusion model directly. Only a few of them showed good correlations therefore new equations were derived empirically from our set of data. All of them have the mathematical formulation: $y=ax^b$

where x is v_p, y is *UCS*, coefficient a covers the petrographic code and exponent b covers the influence of the pore space (porosity/fractures). The derived equations are summarized in Table 1.

	UCS-v_p	R^2
Sandstone	2E-9*v_p^2.91	0,628
Limestone	4E-12*v_p^3.57	0,888
Gypsum/Anhydrite	1E-19*v_p^5.51	0,786

Table 1: derived equations for the correlation between v_p and *UCS* and the resulting regression coefficient.

2.3.2 Defect Model

The second approach for the correlation between v_p and *UCS* is the defect model. This model was published by Schoen (2015). The defect parameter in a solid matrix is characterized by its relative length D (Figure 2). This parameter D summarizes all fractures, pores and cracks.

As a first approximation and using only linear terms the decrease of parameters caused by defects (fractures, cracks) can be described as follows for a dry rock:

$$v_{p,rock} = v_{p,s} \cdot \sqrt{1-D} \quad (6)$$

$$UCS_{rock} = UCS_s \cdot (1-D) \quad (7)$$

$v_{p,s}$ and UCS_s are the values for the compressional wave velocity and uniaxial compression strength of the solid matrix material (host material). For the relationship between *UCS* and elastic wave velocity v_p the simple equation results in

$$UCS_{rock} = v_{p,rock}^2 \cdot \left(\frac{UCS_s}{v_{p,s}^2}\right) = v_{p,rock}^2 \cdot A_s \quad (8)$$

$v_{p,s}$ and UCS_s are the values for the compressional wave velocity and uniaxial compression strength of the solid matrix ma-

	Inclusion model				Defect model		
	Grain density	k_s	μ_s	α	$v_{p,s}$	UCS_s	A_s
	g/cm³	MPa	MPa	-	m/s	MPa	-
Sandstone	2,65	3,8	2	0,1	5000	90	3,60E-06
Limestone	2,75	6,5	2,5	0,1	6500	80	1,90E-06
Gypsum/Anhydrite	2,85	6,2	3,3	0,2	6000	40	1,11E-06

Table 2: Input parameters for the two models applied. Grain density is in gcm^{-3}, k_s and μ_s are in MPa, $v_{p,s}$ in ms^{-1} and UCS_s in MPa. α=aspect ratio, A_s=solid matrix value for the defect model.

terial; $v_{p,rock}$ and UCS_{rock} refer to the compressional and wave velocity of the complete rock including minerals and pores. The rock type is expressed as the parameter A_s (solid matrix value), which is controlled only by mineral composition and properties (same position as host material in case of inclusion models). This solid matrix value (A_s) covers the petrographic influence needs to be determined or defined for the calculations of the defect model. Same input values for elastic properties, depending on rock type, as for the inclusions model are used (Table 2). Additionally, the resulting A_s can be found in Table 2.

3. Results and interpretation

At the beginning of this chapter a short summary about the measured data from the geomechanical and petrophysical laboratory is presented:

- Three limestone types show various porosities, various densities and therefore varying v_p. *UCS* is between 22 and 126 MPa. "Leitha" limestone shows the highest porosities and the lowest *UCS* and v_p values and is taken on the surface in contrast to the other two types of limestone.
- Five sandstone samples show high porosities between 12 and 24 % and low velocities. UCS is low for the sandstone from the Hall Formation (also highest porosity). The other two show similar results than the highly porous "Leitha" limestone.
- Gypsum and anhydrite show both low porosity (around 2 %) and varying values of *UCS* and velocity.

Differences of velocities from the petrophysics laboratory and the ones measured during the uniaxial compression test (Table 3) are mainly the result of different applied forces. In the petrophysics laboratory pressures of about 3 bar are used for the measurements of vp and vs. Higher forces (like applied with the uniaxial compression test) result in higher velocities because of the closure of fractures and cracks. For the correlations the velocities during the uniaxial compression test are used.

The first figure in this chapter (Fig. 3) shows the correlation between v_p and *UCS*. Dots show measured data, which were derived during the uniaxial compression test. The lines were calculated with the petrographic coded model concept (inclusion model) (v_p) and afterwards with the empirically derived correlation equations (*UCS*). Lines start on the right hand side with zero porosity, which increases along the lines. Presented are with grey triangles the sandstone samples, black dots show limestone and light grey cubes gypsum and anhydrite. Sandstone and gypsum/anhydrite show good correlation with the applied model lines and can demonstrate the correlation between v_p and *UCS*. The two limestone values which show the highest v_p cannot be described optimally using the derived equation. These two limestone samples are from the same well and show higher grain and bulk density as well as lower effective porosity than the other two limestone samples. Combining gypsum and anhydrite works well, even if they have a different grain density, they show similar velocities and lower porosities.

Figure 4 shows the same correlation of v_p and *UCS* but here the lines are calculated with the defect model. *UCS* and v_p are presented in logarithmic scale as previously shown like in the literature (Schoen, 2015). The sandstone line can describe only three of the four sandstone samples. This outlier shows the highest effective porosity. Five limestone samples can be described with this defect model. The two outliers show higher *UCS* and also highest velocities. These are the same outliers than in figure 3 with lower porosity and higher grain and bulk density. The same problem occurs for the gypsum and anhydrite. The line can describe two samples, which show lower *UCS*. The third one cannot be reached and would fit to the limestone data even that it is a gypsum sample. This gypsum sample has the highest density and the lowest porosity of all three samples. Comparing this figure with the already published data by Schoen (2015), results fit to each other. Limestone presenter there show a A_s between 3 and 1.2*10^-6 MPa/(ms-1).

Comparing the two model approaches, it can be said that both model types deliver good correlations and are easy applicable, which is important in practice. Inclusion model fits better to the data and reaches

	Uniaxial Compression Test			Petrophysics laboratory			
	vp	vs	UCS	rho	vp	vs	phi
Leitha limestone	3783	2014	22,34	1,75	2990	1986	31,62
Leitha limestone	4306	2370	29,79	1,76	2969	1857	32,84
Leitha limestone	3808	2042	27,21	1,74	3170	1738	34,3
Lithothamium Limestone	4634	2393	45,21	2,43	3243	2286	6,66
Lithothamium Limestone	5125	2936	44,95	2,43	3243	2286	6,66
Lithothamium Limestone	5323	3072	101,95	2,56	4747	2398	10,11
Lithothamium Limestone	5434	3136	126,74	2,57	4631	2416	5,33
Anhydrite	4672	2696	28,7	2,34	4450	2414	2,59
Gyps	4884	2592	20,2	2,26	3800	2172	1,75
Gyps	5716	3139	72,28	2,9	4500	2265	1,5
Sandstone Limnic Series	2854	1606	31,42	2,33	1764	1139	18,57
Buntsandstone	3235	1682	23,08	2,34	1622	1145	11,53
Sandstone Hall Formation	2675	1493	13,48	2,03	1219		23,7
Sandstone Limnic Series	2649	1480	22,72				
Sandstone Puchkirchner Formation	3703	2224	56,2	2,1	2808	1634	13,96

Table 3: measured data during the uniaxial compression test and in the petrophysics laboratory, v_p= compressional wave velocity (ms^{-1}), vs= shear wave velocity (ms^{-1}), UCS=uniaxial compression strength (MPa), ρ=bulk density dry (gcm^{-3}), Φ=effective porosity (%).

nearly all measured data in contrast where the defect model has some outliers. Additionally the defect model verifies the results due to the fact that the data fit to already published data (Schoen 2015).

4. Application on log data

UCS information in the borehole is of great interest for drilling and completion but also in tunnelling and mining, where it helps to calculate risk properties. For the application of the derived equations, two set of logs are selected. Samples from this study were taken from these boreholes. Therefore, the same lithology is given. Applied are for comparison the equations derived from the inclusion and defect model. These equations cover the petrographic code, including lithology influence and porosity information.

Presented in figure 5 a and b are two log sections where cores are taken and measured in the laboratory. *UCS* is calculated with derived correlation equations from the inclusion and defect model. Going into detail about the singular logs presented: Presented are in the first track gamma ray and caliper log. The caliper log gives information about the borehole geometry (measures the diameter of the borehole) and give furthermore information about the technical condition. A caliper log with low values mean that no break outs are observable and that data can be used. Otherwise other measurements can be influenced by the borehole geometry/break outs and the data would need a correction. Gamma ray shows natural radioactivity and gives information about the shale content. Both show in the limestone section low values.

The second track shows depth and limestone, which is presented in blue. Third track presents v_p data, neutron porosity and bulk density. All three logs show a similar shape and the different level clearly separates shale (low velocity, low density, high neutron-porosity) from carbonate rock (high velocity, high density, low neutron-porosity). Because density and neutron-porosity are limestone-scaled the good fit of the curves indicate a water-bearing limestone. Nearly parallel fluctuations of the two logs and the velocity are caused by a variation of limestone porosity.

UCS and v_p decrease with increasing porosity and increasing shale content. The porosity influence is also observable for the laboratory data and is covered with the correlation equations. The last track shows *UCS* data from defect and inclusion model. Additionally presented are the two core samples for each section as black dots. A mean value of *UCS* of 59MPa is calculated for the "Sch" borehole and 86 MPa for the second ("MS") well, resulting from the inclusion model. Core data for the "Sch" well show slightly higher values than the calculated values but are still in the same range. This is maybe a result from the gamma ray, because compared to the "MS" well gamma ray scatters more in the limestone section and shows slightly higher values at some parts. The results for the "MS" well are better, where cores fit well to both calculated "*UCS* logs".

Summarized results for the log sections are:

- Elastic properties give the possibility for correlation with geomechanical properties.
- *UCS* for the defect model is a little bit lower and shows not such a strong influence on vp variations than the results from the inclusion model.
- Both can give indirectly (using a sonic log to calculate *UCS* with derived correlations from the laboratory) information about geomechanical properties.
- *UCS* from both logs show similar results.

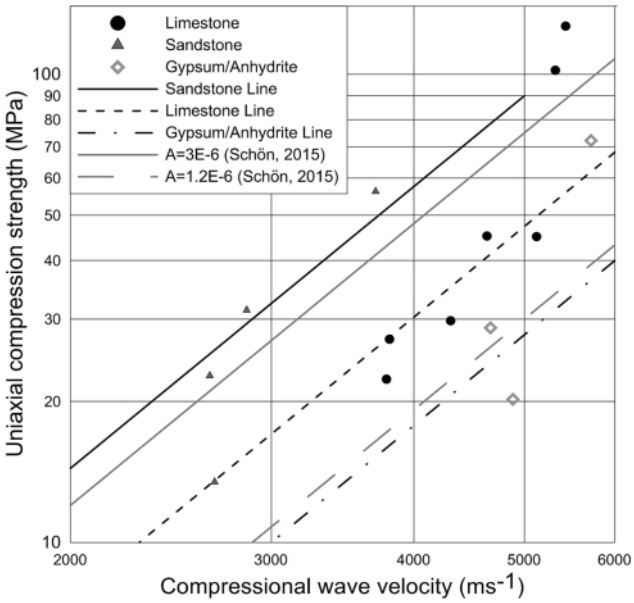

Figure 3: Correlation between compressional wave velocity and uniaxial compression strength, dots are measured data, lines are calculated with the petrographic coded model concept.

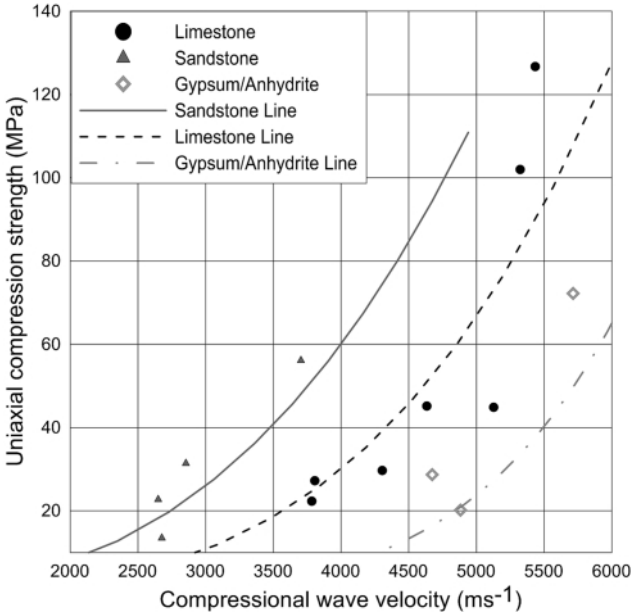

Figure 4: correlation between compressional wave velocity and uniaxial compression strength, dots are measured data, lines are calculated with the defect model, Asandstone=3.6*10^-6; Alimestone= 1.9*10^-6, Agypsum/anhydrite=1.1*10^-6, additionally plotted in grey: lines presented by Schoen (2015).

- *UCS* values from both models compared with core data show excellent results for MS and good results for Sch.

5. Conclusion

The newly developed experimental set-up with compression platens including integrated ultrasonic probes allows determining compressional and shear wave velocities at various stress and strain states. Therefore, the laboratory data become better comparable with log data and furthermore the derivation of geomechanical parameters from geophysical measurements becomes possible. The presented correlations using the petrographic coded model concept shows good first results. The petrographic code is included with the separation of data concerning their rock type and the input for the correlations concerning their petrography. It must be cited that the values are indirectly (correlations from laboratory applied on log data to derive *UCS*) derived and therefore give a kind of mean value for the *UCS* in the formation and a hint about the value. Often no cores are available to make direct measurements.

Measurements and their correlations indicate different behaviour of the rock types:

- Correlation between *UCS* and v_p can be derived with the petrographic coded model concept
- Petrographic coded model covers on the one hand the lithology/rock type influence (petrographic code), which is included using various correlation equations for the singular rock types. On the other hand it covers the pore influence with the inclusions/defects.
- Taking the mineralogical information (petrographic code) is essential for the correlations, because the correlations are dependent on the lithology (geological situation)
- Both approaches (defect and inclusions model) deliver good results with power equations for the correlation between *UCS* and v_p. Recommendation for choosing one of those cannot be given. Probably further studies can help.

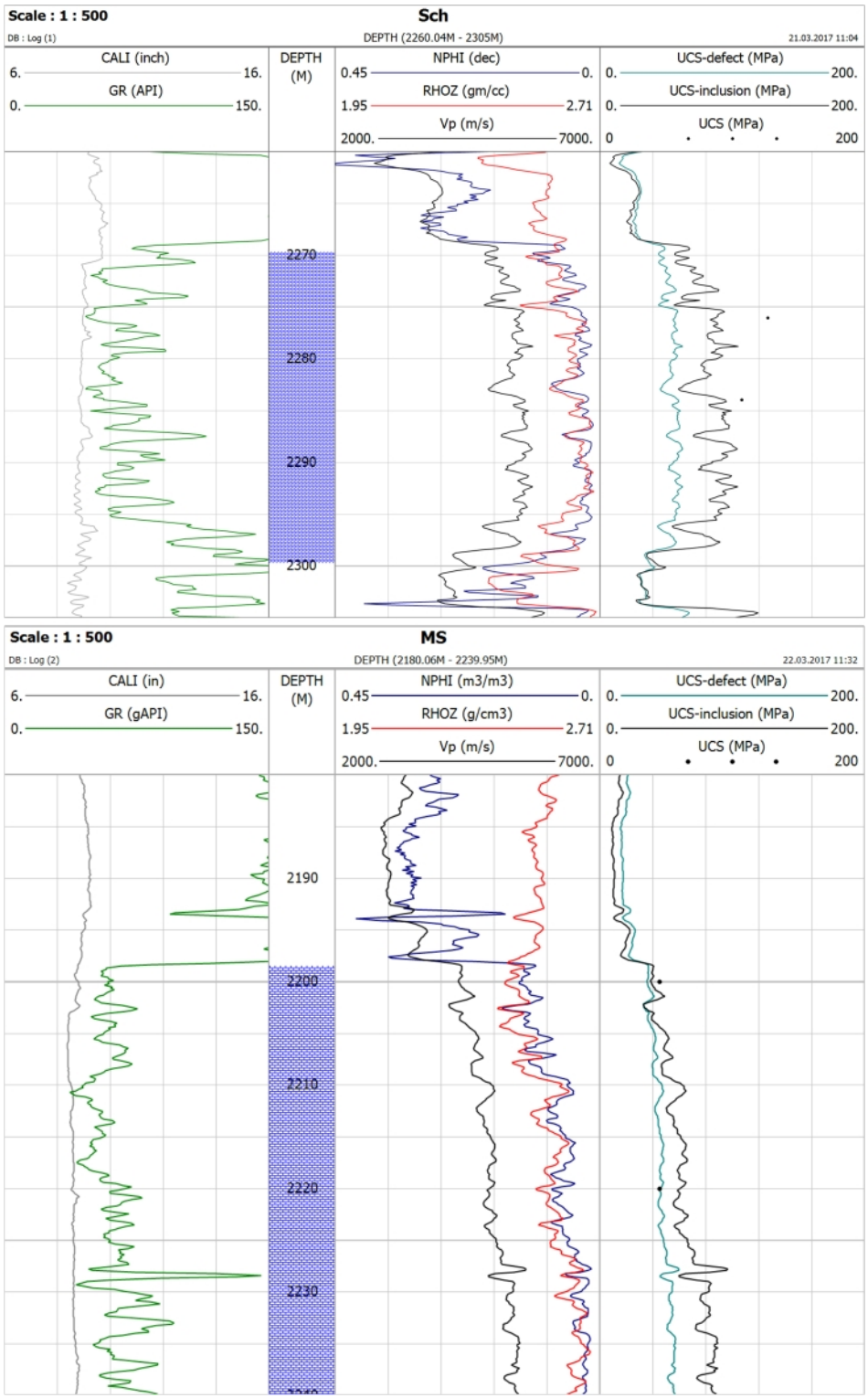

Figure 5: Two log sections for limestone (Sch (2260-2305m) and MS (2180-2240m)). Presented are in the first track, gamma ray and caliper log, second track gives the depth and lithology, the third track shows neutron porosity, vp and density and the fourth track shows UCS from defect model, inclusion model and in dots the values measured in the geotechnical laboratory.

- Equations are easy applicable on log data.
- Log data deliver good results.

At the moment new measurements are carried out including further rock types. The next step will also focus on the application during a triaxial compression test.

References

Altindag, R., 2012. Correlation between P-wave velocity and some mechanical properties for sedimentary rocks. The Journal of the Southern African Institute of Mining and Metallurgy, 112, 229-237.

Bhuiyan, M.H., Holt, R.M. and Fjaer, E., 2013. Anisotropic parameters of dry and saturated sand under stress. SEG Annual Meeting, Houston, 2836-2840.

Budiansky, B. and O'Connell R.J., 1976. Elastic moduli of a cracked solid. International Journal of Solids and Structures, 12, 81-97. https://doi.org/10.1016/0020-7683(76)90044-5

Chang Ch., Zoback, M.D. and Khaksar, A., 2006. Empirical relations between rock strength and physical properties in sedimentary rocks. Journal of Petroleum Science and Engineering, 51, 223-237. https://doi.org/10.1016/j.petrol.2006.01.003

Chen, H. and Hu Z.-Y., 2001. A preliminary study on the relationship between engineering properties and uniaxial compressive strength of weak sandstones. Western Pacific Earth Sciences, 1, 297-338.

Fjaer, E., Holt, R.M., Horsrud, P., Raaen, A.M. and Risnes, R., 2008. Petroleum Related Rock Mechanics. Elsevier Science. 514pp.

Fortin, J., Schubnel, A. and Gueguen, Y., 2005. Elastic wave velocities and permeability evolution during compaction of Bleurswiller sandstone. International Journal of Rock Mechanics & Mining Sciences, 42, 873-889. http://dx.doi.org/10.1016/j.ijrmms.2005.05.002

Gegenhuber, N. and Schoen, J.H., 2012. New approaches for the correlation between compressional wave velcoity and thermal conductivity. Journal of Applied Geophysics, 76, 50-55, http://dx.doi.org/10.1016/j.jappgeo.2011.10.005

Gegenhuber, N. and Schoen, J.H., 2014. Thermal conductivity estimation from elastic wave velocity – application of a petrographic coded model. Petrophysics, 55, 51-56.

Gegenhuber, N. and Kienler, M., 2017. Improved Petrographic Coded Model and its Evaluation to Determine a Thermal Conductivity Log. Acta Geophysica, Volume 65, p 103-118. http://dx.doi.org/10.1007/s11600-017-0010-4

Gegenhuber, N. and Steiner-Luckabauer, C., 2012. Vp/Vs Automatic Picking of Ultrasonic Measurements and their Correlation of Petrographic Coded Carbonates from Austria. 74th EAGE Conference & Exhibition, Copenhagen.

Heerden, W.L., 1987. General Relations between static and dynamic moduli of rocks. International Journal of Rock Mechanics and Mining Sciences and Geomechanics, 24, 381-385. https://doi.org/10.1016/0148-9062(87)92262-5

Hongkui, GE, Yingsong, L., Shanzhou, M. and Lili, S., 2001. Differences of rock elastic parameters under static and dynamic loading. In: ISRM International Symposium - 2nd Asian Rock Mechanics Symposium, Frontiers of rock mechanics and sustainable development in the 21th century, 69-71.

Jiang, J. and Sun, J.-Z., 2011. Comparative study of static and dynamic paramters of rock for the Xishan Rock Cliff Statue. Journal of Zhejiang Univerisity-Science A, 12, 771-781, http://dx.doi.org/10.631/jzus.A1100003

Karami, M., Abrah, B., Dayani, S., Framarzi, L. and Nik, M.G., 2012. Empirical Correlations between Static and Dynamic Properties of intact rock. 7th Asian Rock Mechanics Symposium, Seoul, South Korea.

Mashinskii, E., 2004. Variants of the strain-amplitude dependence of elastic wave velocities in rocks under pressure. Journal of Geophysics and Engineering 1, 295-306. http://dx.doi.org/10.1088/1742-2132/1/4/008

Mavko, G., Mukerji, T. and Dvorkin, J., 2009. The Rock Physics Handbook. Cambridge University Press. 511pp.

Najibi, A.R., Ghafoori, M., Lashkaripour, G.R. and Asef, M.R., 2015. Empirical relations between strength and static and dynamic elastic properties of Asmari and Sarvak limestone, two main oil reservoirs in Iran. Journal of Petroleum Science and Engineering, 126, 78-82, http://dx.doi.org/10.1016/j.petrol.2014.12.010

Pittino, G., Gegenhuber, N., Reiter, F. and Fröhlich, R., 2015. Axiale Prüfkörperdurchschallung während einaxialer Druckversuche. Berg- und Hüttenmännische Monatshefte, 160, 565-571. http://dx.doi.org/10.1007/s00501-015-0423-9.

Oyler, DC, Mark, C. and Molinda, GM., 2008. Correlation of Sonic Travel Time to the Uniaxial Compressive Strength of U.S. Coal Measure Rocks. Proceedings of the 27th International Conference on Ground Control in Mining, July 29 - July 31, Morgantown, West Virginia.

Plona, T. J. and Cook, J. M., 1995. Effects of stress cycles on static and dynamic Young's moduli in Castlegate sandstone. Proceeding of the 35th U.S. Rock Mech. Symp., Reno, Nevada.

Schoen, J.H., 2015. Physical Properties of Rocks - Fundamentals and Principles of Petrophysics. Pergamon. 512pp.

Received: 16 January 2017
Accepted: 31 March 2017

Nina GEGENHUBER[1)*)], Thomas SCHIFKO[2)] & Gerhard PITTINO[3)]

[1)] Montanuniversitaet Leoben, Chair of Applied Geophysics, Franz-Josef-Strasse 18, 8700 Leoben, Austria;

[2)] Fugro Austria GmbH, Einoedstrasse 13, 8600 Bruck an der Mur, Austria;

[3)] Montanuniversitaet Leoben, Chair of Subsurface Engineering, Franz-Josef-Strasse 18, 8700 Leoben, Austria;

[*)] Corresponding author, nina.gegenhuber@unileoben.ac.at